Viscoelasticity of Brownian Carbon Nanotubes in PDMS Semidilute Regime

Sandrine Marceau,[†] Philippe Dubois,[†] René Fulchiron,[‡] and Philippe Cassagnau*,[‡]

Center of Innovation and Reseach in Materials & Polymers (CIRMAP), Laboratory of Polymeric and Composite Materials, University of Mons-Hainaut, Place du Parc 20, B-7000 Mons, Belgium, and Université de Lyon, Lyon, F-69003, France, Université de Lyon 1, Lyon, F-69622, France, CNRS UMR5223, Ingénierie des Matériaux Polymères: Laboratoire des Matériaux Polymères et Biomatériaux, F-69622 Villeurbanne, France

Received November 25, 2008
Revised Manuscript Received January 30, 2009

Introduction. Carbon nanotubes (CNTs) have attracted a huge scientific and technological interest due to their specific properties. CNTs can be viewed as one-dimensional nanomaterial as they possess a very high aspect ratio (nanoscale diameter and microscale length), Young modulus, and electrical conductivity. Consequently, numerous manufacturing applications based on polymeric materials, such as electrostatic painting, protective coating, or flame-resistant composites, have been found at relatively tiny CNT concentrations. However, the successful development of CNT-based composites requires controlling the dispersion of CNTs within the polymer matrix. Indeed, CNTs have a strong tendency to agglomerate in densely packed bundles, and different strategies have been then developed to optimize CNT dispersion in, e.g., thermoplastic polymers. A direct consequence of the incorporation of CNTs in molten polymers is the significant change in the viscoelastic properties. Understanding the viscoelastic properties of nanocomposite thermoplastic polymers is of importance to get a fundamental knowledge on the process ability of these materials. At the same time, viscoelastic properties in the molten state are generally useful to determine the structure−properties relationships of nanocomposites materials.[1] As the filler dispersion, interparticle interaction and the polymer−filler interaction can strongly influence both linear and nonlinear viscoelastic responses; rheology consequently appears to be a unique technique for the study of CNT nanocomposites.[2]

In well-dispersed nanocomposites, the large aspect ratio of CNTs (generally higher than 100) leads to the formation of a solidlike material at a relatively low nanotube concentration. Generally, this concentration onset, at which the linear properties dramatically change with obeying scaling law, is referred as the percolation threshold p_c. From an application point of view, the improvement of the CNT nanocomposite properties stems from its network structure due to the formation of CNT physical bonds. Furthermore, beyond this percolation threshold a fractal nanotube network arises and dominates the rheological responses[3−12] and electrical properties.[5,8,11,13−15] Compared to these studies, less attention has been paid to the rheological behavior of CNT suspension below or near this percolation threshold, i.e., diluted suspensions where nanotubes behave as Brownian rods. However, some breakthrough articles have been reported on the shear behavior of carbon nanotube suspensions. Davis et al.[16] investigated the phase behavior and rheology of single-wall CNTs (SWNTs) dispersed in superacids from dilute to concentrated (or nematic) regimes. Fry et al.[17] studied the anisotropy of SWNTs (purified through thermal oxidation in acids) sheared in a semidilute suspension of low molar mass polyisobutylene. Note that this work was extended to sticky nanotube suspensions by Hobbie and Fry.[18] The main conclusion of these works is that carbon nanotubes are mesoscale analogues of rigid-rod polymers as predicted by the Doi−Edwards theory.[19] Surprisingly enough, some works[8,10] reported a reduced viscosity of polymer/CNT composites at low nanotube concentrations. This apparent violation of the Einstein law was discussed by Tuteja et al.[20] in terms of modification of the longest relaxation times (constraint release mechanism) induced by the presence of nanoparticles.

This poor state of the art regarding the dilute CNT suspension in polymeric matrix originates from different items: (i) the difficulty to reach a CNT fine dispersion at the individual nanotube level, (ii) the poor sensitivity of rheometer and/or the CNT relaxation time longer that the experimentally accessible one, and finally (iii) the rather limited industrial interest for such diluted suspensions. Recently, Beigbeder et al.[21] showed that the addition of 0.5% of "self-pure" multiwall carbon nanotubes (MWNTs) into silicone matrix leads to the spectacular change in the physical and rheological behavior of the recovered nanocomposite materials. On the basis of molecular dynamic simulations, the authors accessed at the microcopic level the adsorption properties of polydimethylsiloxane chains (PDMS) on the external wall surface of MWNTs. They finally demonstrated that the physical adsorption of the PDMS chains onto the CNT wall is mostly triggered by CH−π interactions between part of the PDMS methyl groups and the π-electron-rich surface of CNTs. Such interactions are favorable to CNT dispersion in PDMS at the level of individual CNT as the nanotubes are stabilized against aggregation by the PDMS chain adsorption. Consequently, PDMS/MWNT nanocompositions represent a relevant system to study the case of semidilute suspensions based on CNTs.

Accordingly, the objective of the present paper is to investigate the linear viscoelasticity of diluted suspension of MWNT spread in PDMS. Specifically, we focus our attention on both the CNT relaxation in semidilute conditions and the concept of percolation threshold for such system. Finally, the results, and mainly the concentration dependence of the zero-shear viscosity and mean relaxation time, will be discussed within the Doi−Edwards theory framework on molecular dynamic of rigid rods in a semidilute regime.

Experimental Section. *Materials.* Multiwall carbon nanotubes with a diameter of ca. 10 nm, average length of ca. 1.5 μm, and a minimum purity of 90% (see Table 1) were investigated in this study. These MWNTs have never undergone any surface treatment after being produced by CCVD and were

Table 1. Main Properties of Multiwall Carbon Nanotubes Used in the Present Study

properties	characterization	methods of measurement
average diameter	10 nm	TEM
average length	1.5 μm	TEM
carbon purity	<90%	TGA
surface area	250−300m^2	BET

* To whom correspondence should be addressed. E-mail: philippe.cassagnau@univ-lyon.fr.
[†] University of Mons-Hainaut.
[‡] Université de Lyon 1.

10.1021/ma802628q CCC: $40.75
Published on Web 02/17/2009

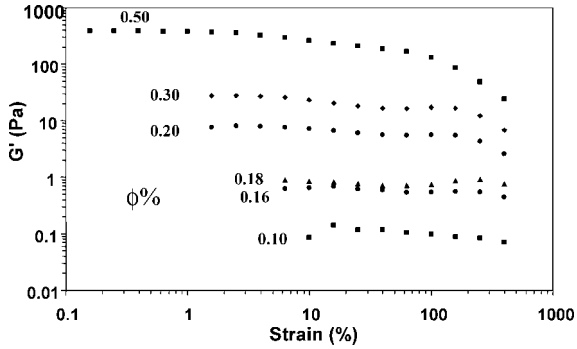

Figure 1. Determination of the linear domain: Strain sweep experiments at $\omega = 1$ rad s^{-1}.

directly used as masterbatch predispersed in PDMS (containing 0.5 wt % in MWCNTs) using a high-shear industrial dispersion process and supplied under Biocyl 2000 trade name by Nanocyl SA (Sambreville, Belgium).

Polydimethylsiloxane (PDMS) Sylgard 184-Part A (from Dow Corning) was used as silicone sample. The number-average molar mass of this PDMS sample is $M_n = 32\,000$ g mol^{-1}. According to the literature,[22,23] this molar mass is close to the critical molar mass for the viscosity $M_c \approx 30\,000$ g mol^{-1}. Practically, Biocyl and Sylgard 184-Part A were mechanically mixed (1200 rpm) for 30 min at room temperature and used without any further mechanical treatment.

Rheology. The viscoelastic experiments were carried out on an ARES rheometer at room temperature ($T \approx 22$ °C). The measurements were then performed in an oscillatory shear mode using a parallel plate geometry with a diameter of 25 mm. Specimens were placed between the plates and were allowed to equilibrate for 48 h prior to each frequency sweep run. This rest time was imposed to allow the sample for recovering its Brownian equilibrium after the deformation stored during preparation and placement between the plates.

Frequency sweeps in the range 0.001−500 rad s^{-1} were applied at low strain. Adding colloidal fillers to polymers affects the nonlinear behavior and time-dependent properties. For example, the effect of strain dependence of the dynamic viscoelastic properties of filled polymers is well-known and often referred to as the Payne effect. Figure 1 shows the variation of the storage modulus versus the strain applied (at $\omega = 1$ rad s^{-1}). As expected, the linear domain decreases with increasing MWNT concentration. However, a strain of 1% is the right balance between torque sensitivity and response in linear domain.

Brownian Nanotubes. The suspension of MWNTs in the PDMS polymeric matrix can be regarded as a solution of long rods with aspect ratio L/d. The molecular dynamics of straight rigid polymer in solution has been theoretically investigated by Doi and Edwards.[19] As expected, the rheology of rods in solution is strongly dependent on rod concentration and aspect ratio. As discussed by these authors, three main regimes of concentration can be discerned. Defining ν as the number of molecules per unit volume of solution:

• Dilute regime ($\nu < 1/L^3$): L^3 is the volume that inside a rod can rotate about its center mass. The rods are then able to rotate freely without any interference interaction with neighboring rods.

• Semidilute regime ($1/L^3 \ll \nu \ll 1/dL^2$): The rods are not able anymore to rotate freely without any interaction from surrounding ones. This transition (dilute/semidilute) occurs when the rod concentration reach a value proportional to$1/L^3$. Therefore, scaling developments[19] showed that the rotational interference becomes significant when

$$\nu \approx \beta/L^3 \tag{1}$$

where β is a dimensionless constant. Experimentally, this constant was found[24] to be roughly close to $\beta \approx 30$.

• Concentrated regime ($\nu > 1/dL^2$): The concentration of the rods is that the rod diameter D is large enough compared to the distance between two consecutive neighboring rods. Consequently, the excluded volume of interaction can no longer be neglected. Just above the onset of this concentrated regime the solution remains isotropic at equilibrium (concentrated isotropic regime). At higher concentration ($\nu > 4.2/dL^2$), the rods can spontaneously orient into a nematic crystalline phase (nematic regime). The molecular dynamic of the rods is no longer Brownian.

According to the volume fraction of rods in solution ($\phi = (\pi/4)d^2L\nu$) the crossover from dilute to semidilute behavior of MWNTs used in the present study is then

$$\phi_0 \approx \frac{30\pi}{4}\left(\frac{d}{L}\right)^2 \tag{2}$$

For an aspect ratio L/d close to 160, the onset of the semidilute regime occurs at ∼0.1% of nanotubes. Furthermore, the onset of the concentrated isotropic regime is

$$\phi_c \approx \frac{\pi}{4}\frac{d}{L} \tag{3}$$

The onset of this isotropic concentrated regime is around 0.5%, and the nematic regime would be higher than 2%.

Regarding the rotary diffusivity D_r of a rod in an isotropic suspension, the Doi−Edwards theory for semidilute regime predicts

$$D_r = AD_{r0}(\nu L^3)^{-2} \tag{4}$$

where D_{r0} is the rotary diffusivity for the rods in dilute solution and A is a dimensionless constant whose values are generally large. From theoretical[25] and simulation[26] considerations the values of this constant have found to be roughly ∼1000 for perfectly rigid rods. On the other hand, the rotary diffusivity in dilute regime[19] is expressed as

$$D_{r0} = \frac{3k_BT(\ln(L/d) - \gamma)}{\pi\eta_m L^3} \tag{5}$$

where k_B is the Boltzmann constant, γ is a constant ($\gamma \sim 0.8$), and η_m is the viscosity of the solvent (or matrix).

Furthermore, the rod concentration dependence of the rotary diffusivity in semidilute suspensions was predicted to be

$$D_r \propto \phi^{-2} \tag{6}$$

And consequently the following power law on zero shear viscosity η_0 and relaxation time τ_r are respectively

$$\eta_0 = \frac{\nu k_BT}{10D_r} \qquad \eta_0 \propto \phi^3 \tag{7}$$

$$\tau_r = \frac{1}{2D_r} \qquad \tau_r \propto \phi^2 \tag{8}$$

The Doi−Edwards theory was actually developed for the predictions of the rheological properties of semidilute isotropic solutions of stiff polymers. An extended theory was developed by Marrucci and Grizzuti[27] to take into account a broad distribution of the rod lengths. However, quantitative agreement between experimental and theory has not been rigorously obtained[28] Even if the rheology of an isotropic rodlike polymer

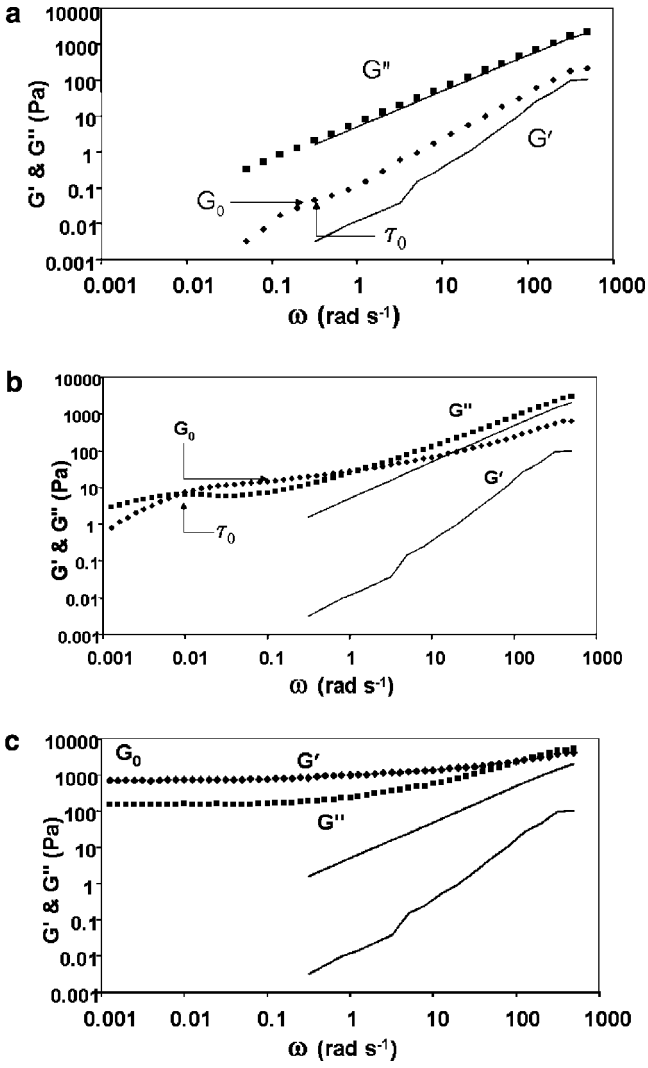

Figure 2. Viscoelastic behavior of MWNT suspensions in PDMS. Variation of the storage and loss moduli (G' and G'', respectively) versus frequency for different MWNT concentrations. $T \approx 22$ °C. The terminal parameters (G_0 and τ_0) of the secondary relaxation are defined in the figures. (a) $\phi = 0.1\%$, (b) $\phi = 0.2\%$, and (c) $\phi = 0.5\%$. The full lines represent the viscoelastic behavior of the neat PDMS matrix.

is still not completely understood,[29] the Doi−Edwards theory turns out to be a relevant theory, at least from a qualitative point of view. For instance, the predicted scaling law on mean relaxation time ($\tau_0 \propto \phi^2$) was observed to be in agreement with experimental observations on flexible collagen molecules.[30] Nevertheless, the Doi−Edwards theory has been rarely applied to semidilute solution of carbon nanotubes. This is mainly due to the difficulties to access the terminal relaxation zone and to proceed with fine dispersion of CNT in solvent or polymer matrix. However, the pioneering works of Fry et al.[31] on rheo-optical studies of carbon nanotube suspensions under shear flow showed that the Doi−Edwards theory can be successfully applied. At least for semidilute suspensions at low Peclet number ($Pe < 200$, $Pe = (4/\pi)^2[(L/D)^4/AD_{r0}]\dot{\gamma}\phi^2$), their results are in agreement with the theory prediction as they observed a leading-order scaling relation for the optical anisotropy such as $Pe^{0.25}$. More recently, Ma et al.[32] developed, in terms of the Doi−Edwards diffusion equation, an "aggregation/orientation" model able to describe the steady shear response of CNT suspensions.

Results and Discussion. Figure 2a−c shows the variations of the complex shear modulus versus the frequency for MWNT concentrations at $\phi = 0.1$, 0.2, and 0.5%, respectively. Three different viscoelastic regimes can be discerned. According to the PDMS molar mass ($M_n \approx 32\,000$ g mol^{-1}) close to the critical molar mass for viscosity ($M_c \approx 30\,000$ g mol^{-1}), the present PDMS sample can be considered as nonentangled. Consequently, the possible effects on the physical interaction between nanotubes and entangled polymer chains are negligible on the rheological behavior of the CNT suspensions. Furthermore, note that G_0 and τ_0 were defined in Figure 2a−c according to a Maxwell model of relaxation. As this second relaxation domain is coupled with the relaxation domain of PDMS at high frequency, the storage modulus G_0 was assessed from the variation of d log G'/d log(ω) according to a method used by Montfort et al.[33] τ_0 was measured from $\tau_0 = 1/\omega_0$, ω_0 being the frequency at the maximum of the viscosity in the Cole−Cole plot of the complex viscosity.

For $\phi = 0.1\%$ (Figure 2a), the terminal relaxation zone is slightly modified compared with pure PDMS matrix. The PDMS chains exhibit typical homopolymer-like terminal behavior ($G' \propto \omega^2$ and $G'' \propto \omega^1$) with the longest relaxation time ($\eta_0 J_e^0$, $J_e^0 \approx (5 \pm 2) \times 10^{-4}$ Pa^{-1}) equal to 2.5×10^{-4} s. The appearance of a second relaxation zone can be observed since a relaxation time (centered around ~5 s) can be defined. This second relaxation zone is due to the physical contacts between MWNTs, which appear at the onset of the transition between dilute and semidilute regimes. Consequently, the concentration $\phi_0 = 0.1\%$ is close to the onset of the semidilute regime according to the theoretical derivation of eq 2 for solid rods ($\nu L^3/\beta \approx 1$). Regarding the determination of the transition from dilute to semidilute regimes, Davis et al.[16] and Parra-Vasquez et al.[34] proposed to use the reciprocal value of the intrinsic visosity ($[\eta_0] = \lim_{\phi \to 0} [(\eta_0 - \eta_s)/\phi\eta_s]$). In the present work, we found $[\eta_0] = 800 \pm 100$ and $\phi_0 = (0.125 \pm 0.02)\%$. This value is close to the theoretical one from eq 2. Furthermore, as derived by the same authors,[16,34] the aspect ratio of the CNTs can be estimated from the intrinsic viscosity. We finally found $L/d \approx 250$. This value is much higher than the value calculated from TEM observation ($L/d \approx 160$). The nanotube length distribution could explain this 35% difference.

For $\phi = 0.2\%$, this second relaxation zone is clearly evidenced. As far as we know, it is the first time that such behavior is reported for carbon nanotube suspensions. For example, Figure 2b clearly depicts the relaxation dynamics of MWNTs associated with their Brownian motions in PDMS matrix. The Peclet number, which is a measure of the relative importance of the Brownian motion and shear-induced deformation, can be expressed as $P_e \propto \omega\gamma_0/D_r$. For $\phi = 0.2\%$, $D_r \approx 5 \times 10^{-5}$ s^{-1} according to eq 4, we obtain $Pe \approx 2$. It can be then assumed that the relaxation of the individual nanotubes by Brownian motions is the primary mechanism for the relaxation process. As a result, a temporary elasticity network G_0 with a relaxation time τ_0 defines this terminal viscoelastic behavior in the semidilute regime.

Upon increasing the MWNT concentration, Figure 2c shows ($\phi = 0.5\%$) that the storage modulus G' is independent of frequency at low frequency, at least in the accessible frequency domain. Note that this behavior is observed (Figure 3) from $\phi = 0.3\%$. This dominance of G' over G'' indicates that the MWNT relaxation time is longer than experimentally accessible, i.e., the low frequency accessible ($\omega = 10^{-3}$ rad s^{-1}). A priori, these concentrations ($\phi = 0.3$ and 0.5%) are far below the isotropic concentrated regime predicted to be 2% from theoretical considerations. However, this statement does not account for polydispersity of CNTs.

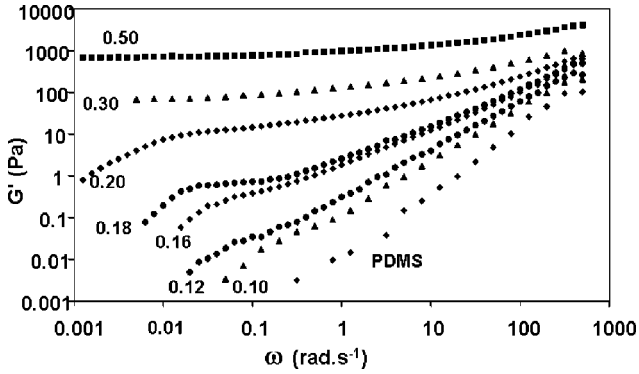

Figure 3. Variation of the storage modulus versus frequency for different MWNT concentrations $\phi = 0.1$, 0.12, 0.16, 0.18, 0.20, 0.30, and 0.50%.

Table 2. Terminal Viscoelastic Parameters of Semidilute MWNT in PDMS ($T \approx 22$ °C) versus NTC Loading[a]

CNT (%)	νL^3	η_0 (Pa s)	τ_0 (s)	G_0 (Pa)	D_r (s^{-1})	A
PDMS		5				
0.10	32	7.5	5	0.03	5.2×10^{-4}	520
0.12	38	10	10	0.05	4.6×10^{-4}	460
0.16	51	40	15	0.3	1.5×10^{-4}	400
0.18	57	60	25	0.8	1.2×10^{-4}	380
0.20	64	200	100	12	5.0×10^{-5}	160
0.30	95			70		
0.50	160			700		

[a] η_0: zero shear viscosity; τ_0: mean relaxation time; G_0: equilibrium modulus; D_r: rotary diffusivity (from eq 4); and dimensionless constant A (from eq 4).

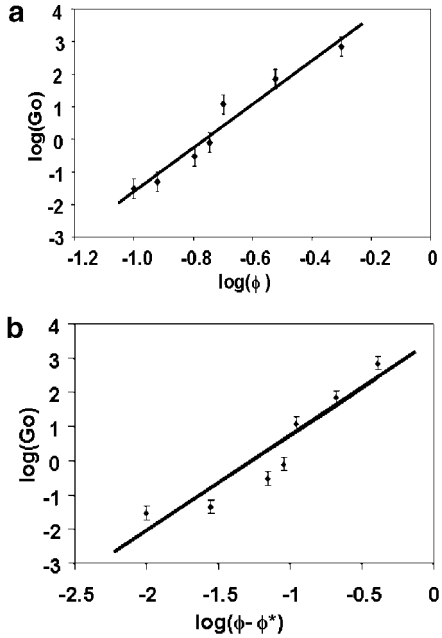

Figure 4. Concentration dependence of the elastic modulus G_0. (a) $G_0 \propto \phi^{6.7\pm0.2}$. (b) Double-log plot of G_0 versus $(\phi - \phi^*)$. The critical exponent $\alpha = 2.7 \pm 0.2$ has been calculated from this slope.

Figure 3 and values from Table 2 show the secondary plateau modulus greatly jumps by ~5 orders of magnitude between 0.1 and 0.5% ($32 < \nu L^3 < 160$) of MWNT concentration. According to Figure 4a, the plateau modulus G_0 obeys the following power law:

$$G_0 \propto \phi^{6.7\pm0.2} \tag{9}$$

This scaling exponent law is remarkably and surprisingly close to the exponent ($G_0 \propto \phi^{7.1\pm0.3}$) observed by Hobbie and Fry[18,35] for nanotube suspension in the regime $100 < \nu L^3 < 2500$. On the other hand, the physical network caused by the nanotube interactions has been interpreted in terms of percolation at the transition between the dilute and semidilute regimes.[4] Near the critical transition, the storage modulus G_0 behaves according to the following scaling law:

$$G_0 \propto (\phi - \phi^*)^{\alpha} \tag{10}$$

where ϕ^* is the critical concentration and α is the scaling exponent. From the double-log plot of G_0 versus $(\phi - \phi^*)$ by varying ϕ^* to minimize the error in the slope in Figure 4b, we obtain $\phi^* = 0.009\%$ and $\alpha = 2.7 \pm 0.2$. The concentration $\phi^* = 0.09\%$ is very close to the critical concentration between the dilute and semidilute regimes of MWNTs as theoretically derived from the Doi−Edwards theory (eq 2) and experimentally observed from viscoelastic measurements ($\phi_0 = 0.1\%$) and intrinsic viscosity ($\phi_0 = 0.125\%$). Regarding the scaling law on the elastic modulus, an exponent $\alpha = 2.3 \pm 0.1$ has been already reported by Hough et al.[4] for single wall carbon nanotube suspensions in water for the NTC concentration regime ($86 < \nu L^3 < 860$). Referring to simulations of percolating network,[36] these authors came to the conclusion that the nanotube network is composed of freely jointed, associating rods. Our results are in agreement with this conclusion; i.e., the nanotubes in the semidilute regime can be considered as Brownian identities.

Nevertheless, the dramatic change of viscoelastic behavior with MWNT concentration of PDMS suspensions cannot be explained from the framework of fractal network[37] generally associated with the percolation theory. Indeed, the network elasticity resulting from the nanotube interactions appears to be a temporary elasticity like in entangled polymers. Figure 2b clearly demonstrated this argument. On the other hand, the fractal criterion of self-similar relaxation as defined by Winter and Mours[37] cannot be applied to the present system. At the liquid−solid transition, this criterion postulates that the shear relaxation module behaves as $G(t) \propto St^{-n}$, and consequently the complex shear modulus should obey the power law $G'(\omega) \propto G''(\omega) \propto \omega^n$. There is no evidence for such a transition from liquidlike to solidlike behavior as observed for some polymer nanocomposites.[1,38] However, a fractal structure is generally reported in the literature[39] for carbon nanotube suspensions. These suspensions are characterized by non-Brownian clusters (or flocs) of nanotubes with a characteristic size of few micrometers. We believe that in our case the dominance of nanotube clusters should appear at the transition between semidilute regime and concentrated isotropic regime ($\phi \approx 2\%$). As discussed below, the power laws on viscosity and relaxation time showed that nanotubes clustering becomes effective at concentration higher than 0.3%. To conclude this part, the percolation concept cannot be strictly applied to our system in the concentration regime ($32 < \nu L^3 < 160$) characterized by a temporary elasticity network of Brownian nanotubes. Surprisingly, the critical exponents are however found to be close to exponents of suspensions characterized by a permanent elastic network of non-Brownian nanotubes ($100 < \nu L^3 < 2500$).

Finally, Figure 5a,b shows respectively the variation of the zero shear modulus and mean relaxation time as a function of the MWNT concentrations ($0.1 < \phi\% < 0.5$). The predicted scaling laws $\eta_0 \propto \phi^3$ and $\tau_0 \propto \phi^2$ are reported in these figures, respectively. Note that the mean relaxation time, as defined from viscoelastic curves, is proportional to the rotary relaxation time ($\tau_0 = (\nu L^3)^2 \tau_r$). It can be then observed than the deviation from the theoretical scaling dramatically increases with MWNT loading. Quantitatively and according to eq 7, the rotary

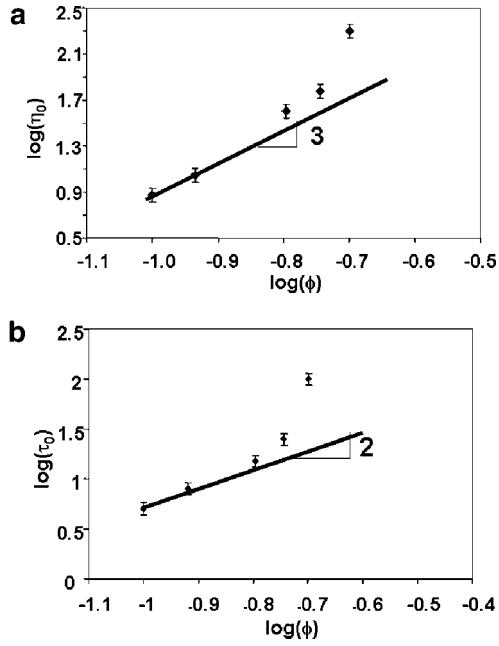

Figure 5. Variation of the zero shear viscosity η_0 and mean relaxation time τ_0 versus MWNT concentration. The full lines are the prediction of the power law from Doi−Edwards theory: (a) $\eta_0 \propto \phi^3$; (b) $\tau_0 \propto \phi^2$.

diffusion can be derived so that the dimensionless constant A can be calculated (see Table 2). Surprisingly, A varies monotonically from $A \approx 520$ for $\phi = 0.1\%$ to $A \approx 160$ for $\phi = 0.2\%$. The value $A \approx 520$ is in the same order of magnitude of predicted and experimental values for rigid rods ($A \approx 1000$). However, the fact that A decreases with increasing nanotube concentration means that the rotary diffusion D_r does not rigorously obey the power law $D_r \propto \phi^{-2}$. The rotary diffusion of MWNTs is much more slowed down with the concentration than as theoretically expected. Such a result was recently reported by Ma et al.[32] As clearly explained by these authors, the coefficient A represents the relative rate of disaggregation to aggregation of CNTs. In other words, it is more difficult to disentangle CNTs at high nanotube loading as the interspacing between CNTs decreases upon increasing CNT concentration. Possible CNT clustering with nanotube loading, even if the CNTs can be assumed individually separated at their scale level, can be also argued to explain this phenomenon. The transmission electronic microscopy picture (Figure 6) ($\phi = 0.2\%$) shows that MWNTs are individually separated in the PDMS suspension. However, certain zones of the sample seem to be more concentrated in CNTs more likely due to the formation of some clusters. Finally, the nanotube length distribution could be another possible explanation as discussed by Larson and Mead[28] for concentrated solution of stiff polymers and Fry et al.[31] for CNT suspensions in polyisobutylene of low molar mass.

Conclusion. The objective of the present work is to investigate the effect of multiwall-carbon nanotube concentrations on their viscoelastic behavior in a PDMS suspension. These MWNTs are expected to be individually dispersed in PDMS matrix. The critical transition of the semidilute regime, defined as the appearance of a second relaxation zone or defined as the reciprocal of the intrinsic viscosity, is observed close to the Doi−Edwards theory on the Brownian dynamics of rigid rods. On the other hand, the predicted scaling laws with concentration, $\eta_0 \propto \phi^3$ and $\tau_0 \propto \phi^2$, are observed to hold just above the semidilute transition. The deviation of these scaling laws at higher concentrations is related to a clustering phenomenon of MWNTs that produces additional slowing of the rotational motion. Finally, we believe that a fractal behavior of the nanotubes should be clearly dominant above the onset of the concentrated regime even if clustering is effective at lower concentration ($\phi \approx 0.3\%$).

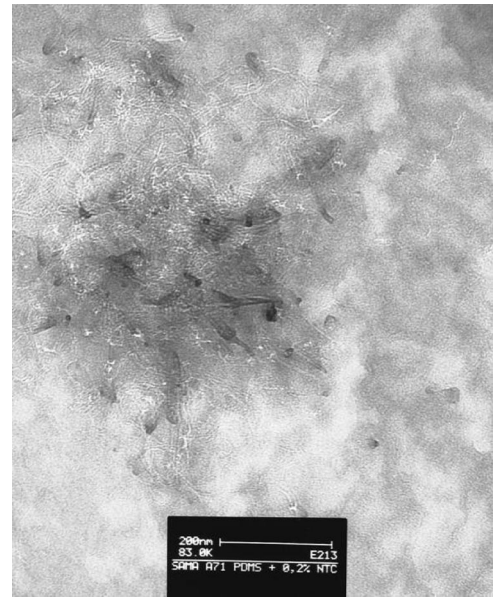

Figure 6. TEM picture of MWNT suspension in PDMS (nanotube content: 0.2 wt %) as recorded over a thin sample slide obtained by ultra-cryomicrotomy.

Acknowledgment. CIRMAP is grateful to "Région Wallonne" for a grant in the frame of the Plan Marshall-MECATECH program: NANOCOMPO project and acknowledges the financial support from the "Région Wallonne" and the European Commission (FSE, FEDER) in the frame of Objectif-1 and Phasing-Out programs. This work was partially supported by the Belgian Federal Science Policy Office (PAI6/27).

References and Notes

(1) Cassagnau, P. *Polymer* **2008**, *49*, 2183–2196.
(2) Zhang, Q.; Fang, F.; Zhao, X.; Li, Y.; Zhu, M.; Chen, D. *J. Phys. Chem. B* **2008**, *112*, 12606–12611.
(3) Mitchell, C. A.; Bahr, J. L.; Arepalli, S.; Tour, J. M.; Krishnamoorti, R. *Macromolecules* **2002**, *35*, 8825–8830.
(4) Hough, L. A.; Islam, M. F.; Janmey, P. A.; Yodh, A. G. *Phys. Rev. Lett.* **2004**, *93*, 168102.
(5) Pötschke, P.; Abdel-Goad, M.; Alig, I.; Dudkin, S.; Lellinger, D. *Polymer* **2004**, *45*, 8863–8870.
(6) Du, F.; Scogna, R. C.; Zhou, W.; Brand, S.; Fischer, J. E.; Winey, K. I. *Macromoloecules* **2004**, *37*, 9048–9055.
(7) Kharchenko, S. B.; Douglas, J. F.; Obrzut, J.; Grulke, E. A.; Migler, K. B. *Nat. Mater.* **2004**, *3*, 564–568.
(8) Zhang, Q.; Lippits, D. R.; Rastogi, S. *Macromolecules* **2006**, *39*, 658–666.
(9) Chatterjee, T.; Krishnamoorti, R. *Phys. Rev. E* **2007**, *75*, 050403.
(10) Wang, M.; Wang, W.; Liu, T.; Zhang, W. D. *Compos. Sci. Technol.* **2008**, *68*, 2408–2502.
(11) Xu, D. H.; Wang, Z. H.; Douglas, J. F. *Macromolecules* **2008**, *41*, 815–825.
(12) Chatterjee, T.; Jackson, A.; Krishnamoorti, R. *J. Am. Chem. Soc.* **2008**, *130*, 6934–6935.
(13) Lima, M. D.; Andrade, M. J.; Skakalova, V.; Bergmann, C. P.; Roth, S. J. *Mater. Chem.* **2007**, *17*, 4846–4853.
(14) Deng, F.; Zheng, Q. S. *Appl. Phys. Lett.* **2008**, *92*, 071902.
(15) Hu, N.; Masuda, Z.; Yan, C.; Yamamoto, G.; Fukunaga, H.; Hashida, T. *Nanotechnology* **2008**, *19*, 215701.
(16) Davis, V. A.; Ericson, L. M.; Parra-Vasquez, N. G. P.; Fan, H.; Wang, Y.; Prieto, V.; Longoria, J. A.; Ramesh, S.; Saini, R. K.; Kittrell, C.; Billups, W. E.; Adams, W. W.; Hauge, R. H.; Smalley, R. E.; Pasquali, M. *Macromolecules* **2004**, *27*, 154–160.

(17) Fry, D.; Langhorst, B.; Kim, H.; Grulke, E.; Wang, H.; Hobbie, E. K. *Phys. Rev. Lett.* **2005**, *95*, 038304.
(18) Hobbie, E. K.; Fry, D. J. *Phys. Rev. Lett.* **2006**, *97*, 036101.
(19) Doi, M.; Edwards, S. F. *The Theory of Polymer Dynamics*; Oxford Press: London, 1986.
(20) Tuteja, A.; Mackay, M. E.; Hawker, C. J.; Van Horn, B. *Macromolecules* **2005**, *38*, 8000–8011.
(21) Beigbeder, A.; Linares, M.; Devalkenaere, M.; Degee, Ph.; Claes, M.; Beljonne, D.; Lazzaroni, R.; Dubois, P. *Adv. Mater.* **2008**, *20*, 1003–1007.
(22) Longin, P.; Verdier, C.; Piau, M. J. *Non-Newtonian Fluid Mech.* **1998**, *76*, 213–232.
(23) Ressia, J. A.; Villar, M. A.; Vallés, E. M. *Polymer* **2000**, *41*, 6885–6894.
(24) Mori, Y.; Ookubo, N.; Hayakawa, R. *J. Polym. Sci., Part B: Polym. Phys.* **1982**, *20*, 2111–2124.
(25) Teraoka, I.; Hayakawa, R. *J. Chem. Phys.* **1989**, *91*, 264362648.
(26) Bitsanis, I.; Davis, H. T.; Tirrell, M. *Macromolecules* **1990**, *23*, 1157–1165.
(27) Marrucci, G.; Grizzuti, N. *J. Non-Newtonian Fluid Mech.* **1984**, *14*, 103–119.
(28) Larson, R. G.; Mead, D. W. *J. Polym. Sci., Part B: Polym. Phys.* **1991**, *29*, 1271–1285.
(29) Larson, R. G. *The Structure and Rheology of Complex Fluids*; Oxford University Press: New York, 1999.
(30) Chow, A. W.; Fuller, G. G.; Wallace, D. G.; Madri, J. A. *Macromolecules* **1985**, *18*, 805–810.
(31) Fry, D.; Langhorst, B.; Wang, H.; Becker, M. L.; Bauer, B. J.; Grulke, E. A.; Hobbie, E. K. *J. Chem. Phys.* **2006**, *124*, 054703.
(32) Ma, W. K. A.; Chinesta, F.; Ammar, A.; Mackley, M. R. *J. Rheol.* **2008**, *52*, 1311–1330.
(33) Montfort, J. P.; Marin, G.; Monge, P. *Macromolecules* **1986**, *19*, 1979–1988.
(34) Parra-Vasquez, A. N. G.; Stepanek, I.; Davis, V. A.; Moore, V. C.; Haroz, H.; Shaver, J.; Hauge, R. H.; Smalley, R. E.; Pasquali, M. *Macromolecules* **2007**, *40*, 4043–4047.
(35) Hobbie, E. K.; Fry, D. J. *J. Chem. Phys.* **2007**, *126*, 124907.
(36) Sahimi, M.; Arbabi, S. *Phys. Rev. B* **1993**, *47*, 703–712.
(37) Winter, H. H.; Mours, M. *Adv. Polym. Sci.* **1997**, *134*, 165–234.
(38) Cassagnau, P. *Polymer* **2003**, *44*, 2455–2462.
(39) Chatterjee, T.; Krishnamoorti, R. *Macromolecules* **2008**, *41*, 5333–5338.

MA802628Q